




## Isogeometric Shape and Topology Optimization of Kirchhoff-Love Shell Structures Using Analysis-Suitable Unstructured T-splines

Wei Wang<sup>1</sup>, Jiaming Yang<sup>2</sup>, Xiaoxiao Du<sup>3</sup> , Pengfei Zhang<sup>4</sup>, Pengfei Han<sup>5</sup>, Yazui Liu<sup>6</sup>, Gang Zhao<sup>7</sup>

<sup>1</sup>School of Mechanical Engineering & Automation, Beihang University, [jrrt@buaa.edu.cn](mailto:jrrt@buaa.edu.cn)

<sup>2</sup>School of Mechanical Engineering & Automation, Beihang University, [williamyj@163.com](mailto:williamyj@163.com)

<sup>3</sup>School of Mechanical Engineering & Automation, Beihang University, [duxiaoxiao@buaa.edu.cn](mailto:duxiaoxiao@buaa.edu.cn)

<sup>4</sup>Research Institute of Aero-Engine, Beihang University, [ftd423@buaa.edu.cn](mailto:ftd423@buaa.edu.cn)

<sup>5</sup>Research Institute of Aero-Engine, Beihang University, [hanpf@buaa.edu.cn](mailto:hanpf@buaa.edu.cn)

<sup>6</sup>Research Institute of Aero-Engine, Beihang University, [liuyazui@buaa.edu.cn](mailto:liuyazui@buaa.edu.cn)

<sup>7</sup>School of Mechanical Engineering & Automation, Beihang University, [zhaog@buaa.edu.cn](mailto:zhaog@buaa.edu.cn)

Corresponding author: Xiaoxiao Du, [duxiaoxiao@buaa.edu.cn](mailto:duxiaoxiao@buaa.edu.cn)

**Abstract.** Structural shape and topology optimization plays a crucial role in the optimal design of shell structures, which are widely used in engineering fields. Isogeometric analysis provides a friendly alternative for the integrated design and analysis of shell structures. This paper developed an isogeometric shape and topology optimization framework for the optimal design of shell structures by using analysis-suitable unstructured T-splines. The Kirchhoff-Love shell theory is employed for structural analysis. The adjoint-based analytical sensitivity analysis is implemented for shape optimization and a smooth density distribution strategy is used for topology optimization. A multi-level scheme is established with a coarse mesh for the design model and a dense mesh for the analysis model. The proposed method is demonstrated by two shape optimization examples and one topology optimization example.

**Keywords:** shape and topology optimization, isogeometric analysis, Kirchhoff-Love shell, adjoint sensitivity

**DOI:** <https://doi.org/10.14733/cadaps.2025.245-260>

## 1 INTRODUCTION

Shell structures have been extensively used in engineering fields, such as aerospace, shipbuilding, automobile, and construction, due to their attractive properties like lightweight, structural stability, and spacial force transmission. Generally, shell structures are defined by small thicknesses and are typically curved along in-plane directions. The design of shell structures is a non-trivial task. An excellent design can increase stiffness

and strength, and reduce material simultaneously. In the past decades, the optimal design of shell structures using numerical tools has been widely investigated and has obtained abundant achievement [26, 3].

The conventional finite element methods (FEMs) have been often utilized to calculate structural responses and sensitivities in the structural optimization process. However, the discretization of smooth shell structures into facet elements will lead to geometric inaccuracy and continuity reduction, which will further affect the effectiveness of structural optimization. In addition, the frequent exchange of geometric data between the design model and the analysis model is time-consuming. Isogeometric analysis, proposed by Hughes and coworkers [16], unifies the geometric representation of the design model and the analysis model, greatly integrating the CAD/CAE process. The spline functions used to represent geometric models in CAD are employed as the shape functions in analysis models for simulations. The sophisticated mesh generation can be tactfully avoided. It provides a friendly alternative for structural optimization besides the conventional FEMs.

In recent years, isogeometric analysis (IGA) has already been used for both structural shape and topology optimization. Seo et al. [32] first studied the NURBS-based isogeometric shape optimization of shell structures based on the Reissner-Mindlin (RM) shell theory. Kiendl et al. [20] proposed a semi-analytical sensitivity analysis and sensitivity weighting method for NURBS-based isogeometric shape optimization of shells based on the Kirchhoff-Love (KL) shell formulation. To handle the complex design domain problems, Bandara et al. [2] used subdivision surfaces for isogeometric structural shape optimization. Kang and Youn [18] considered the topologically complex geometries built with trimmed patches in the shape optimization. Lian et al. [22] combined T-splines and isogeometric boundary element method for shape sensitivity analysis. Hirschler et al. [15] investigated the shape optimization of non-conforming stiffened multi-patch structures. The isogeometric shape optimization has also been applied to the optimal design of composite shells [27, 14, 43, 39, 23]. Moreover, some researchers focused on the calculation of sensitivity [25], optimization algorithms [36], adaptive refinement [6], thickness distribution [7] in isogeometric structural shape optimization. Kang and Youn [19] studied the isogeometric topology optimization of shell structures built with trimmed NURBS patches. Zhang et al. [41] developed an IGA-based moving morphable void method for structural topology optimization. Afterward, they considered stress-related topology optimization of shell structures [40]. Cai et al. [4] combined the IGA method, the adaptive bubble method and the finite cell method for simultaneous shape and topology optimization of shell structures. Pan et al. [29] proposed an IGA-based SIMP method for structural topology optimization based on the Reissner-Mindlin theory.

From the above-reviewed works, isogeometric structural shape and topology optimization usually employs NURBS functions for the representation of the design domain and structural analysis. When considering a complex domain built with multiple NURBS patches, additional works like interface coupling, and dealing with trimming elements are required [8, 9, 11, 10]. In this paper, we developed an isogeometric shape and topology optimization approach using analysis-suitable unstructured T-splines (ASUT-splines), which can greatly alleviate the heavy burden of dealing with complex geometries. The ASUT-splines generalize the definition of analysis-suitable T-splines [21] to allow unstructured T-mesh with extraordinary points [31]. This extension dramatically improves the geometric representation capacity of topologically complex models with a single ASUT-spline patch. To achieve  $C^1$  continuity at the vicinity of extraordinary points, Nguyen and Peters [28] employed the D-patch method which was first proposed by Reif [30]. Toshniwal et al. [34] combined D-patch and a split-then-smoothen strategy for integrated modeling and analysis on unstructured quad meshes. Recently, the ASUT-splines have been extended and applied for isogeometric analysis of complex shell structures [5, 35, 36, 13]. To further extend the capability of complex model representation, Liu et al. [24] utilized a weak coupling method to couple multiple unstructured T-spline patches for large thin shell analysis. Yang et al. [37] developed a surface blending method to blend multiple ASUT-spline patches. Zhao et al. [42] first studied the isogeometric topology optimization of two-dimensional models built with ASUT-splines.

In this paper, we developed an isogeometric structural shape and topology optimization method using ASUT-splines for geometric modeling and structural analysis. The data exchange between design models and analysis models is discussed within the multi-level optimization framework. The Kirchhoff-Love shell

theory is utilized for the calculation of structural responses. The sensitivity formulations in isogeometric shape optimization are derived in detail. In addition, we employed ASUT-splines to construct continuous density functions for isogeometric structural topology optimization. Several numerical examples are implemented to validate the performance of isogeometric structural shape and topology optimization on topologically complex design domains.

## 2 ISOGEOMETRIC KIRCHHOFF-LOVE SHELL FORMULATIONS

The Kirchhoff-Love shell theory is employed for structural analysis. To achieve  $C^1$  continuity over the the vicinity of extraordinary points, non-uniform D-patch [38], Bézier extraction and truncation schemes are utilized. Based on the Kirchhoff-Love assumption, the material point of a shell is expressed as

$$\mathbf{x}(\xi, \eta, \zeta) = \mathbf{s}(\xi, \eta) + \zeta \mathbf{a}_3(\xi, \eta), \quad (1)$$

in which  $\mathbf{s} : \bar{\Omega} \rightarrow \Omega$  indicates the middle surface of the shell structure;  $\zeta \in [-t/2, t/2]$  and  $t$  is the thickness;  $\mathbf{a}_3(\xi, \eta)$  is the unit normal vector defined at the point  $(\xi, \eta)$ . Let  $\mathbf{a}_1 = \mathbf{s}_{,\xi}$ ,  $\mathbf{a}_2 = \mathbf{s}_{,\eta}$  be the two tangent vectors, then the normal vector  $\mathbf{a}_3 = \mathbf{a}_1 \times \mathbf{a}_2 / \|\mathbf{a}_1 \times \mathbf{a}_2\|$ .

By using ASUT-splines, each element of the shell structure can be represented by

$$\mathbf{s}^e(\xi, \eta) = \sum_{a=1}^{m_{cp}^e} \mathbf{q}_a^e R_a^e(\xi, \eta) = \mathbf{R}^e \mathbf{Q}^e, \quad (\xi, \eta) \in \bar{\Omega}^e, \quad e = 1, 2, \dots, m_e, \quad (2)$$

where  $m_e$  is the number of elements in analysis models;  $m_{cp}^e$  is the number of control points corresponding to the element  $e$ ;  $\mathbf{Q}^e$  is a  $3m_{cp}^e \times 1$  column vector consisting of coordinates of control points;  $\mathbf{R}^e$  is written as

$$\mathbf{R}^e = \begin{bmatrix} R_1^e & 0 & 0 & R_2^e & \dots & R_{m_{cp}^e}^e & 0 & 0 \\ 0 & R_1^e & 0 & 0 & \dots & 0 & R_{m_{cp}^e}^e & 0 \\ 0 & 0 & R_1^e & 0 & \dots & 0 & 0 & R_{m_{cp}^e}^e \end{bmatrix}. \quad (3)$$

Under the framework of IGA, the displacement field  $\mathbf{u}(\xi, \eta)$  is discretized as

$$\mathbf{u}^h(\xi, \eta) = \sum_{a=1}^{m_{cp}^e} \mathbf{u}_a^e R_a^e(\xi, \eta) = \mathbf{R}^e \mathbf{u}^e, \quad (\xi, \eta) \in \bar{\Omega}^e, \quad e = 1, 2, \dots, m_e, \quad (4)$$

in which  $\mathbf{u}_a^e$  denotes the displacement vector at the control point  $a$ ;  $\mathbf{u}^e$  indicates the displacement vector of the element  $e$ . The first and second derivatives of  $\mathbf{R}^e$  are denoted by  $\mathbf{R}_{,\alpha}^e$  and  $\mathbf{R}_{,\alpha\beta}^e$ . The subscript  $\alpha$  and  $\beta$  take values 1 and 2. As a consequence, we have  $\mathbf{a}_{\alpha} = \mathbf{R}_{,\alpha}^e \mathbf{Q}^e$  and  $\mathbf{a}_{\alpha,\beta} = \mathbf{R}_{,\alpha\beta}^e \mathbf{Q}^e$ .

Assume that the shell structure undergoes a small deformation, the stiffness matrix and external force vector are given by

$$\mathbf{K}^e = \int_{\Omega^e} \left( \mathbf{B}_m^T \mathbf{D}_0 \mathbf{B}_m + \mathbf{B}_b^T \mathbf{D}_2 \mathbf{B}_b \right) d\Omega^e, \quad (5)$$

$$\mathbf{F}^e = \int_{\Omega^e} (\mathbf{R}^e)^T \mathbf{f} d\Omega^e, \quad (6)$$

where  $\mathbf{B}_m$  and  $\mathbf{B}_b$  are strain-displacement matrices;  $\mathbf{f}$  is the applied force. For an explicit representation of matrices  $\mathbf{B}_m$  and  $\mathbf{B}_b$  we recommend [12] for more details.  $\mathbf{D}_0$  and  $\mathbf{D}_2$  are constitutive matrices and can be represented using the metric components  $g_{ij}$ . Let  $\mathbf{g}_{\alpha}$  be the covariant base vectors defined by

$$\mathbf{g}_{\alpha} = \mathbf{x}_{,\alpha} = \mathbf{a}_{\alpha} + \zeta \mathbf{a}_{3,\alpha}. \quad (7)$$

Then the metric components  $g_{ij}$  are computed as

$$g_{\alpha\beta} = \mathbf{a}_\alpha \mathbf{a}_\beta - 2\zeta \mathbf{a}_{\alpha,\beta} \mathbf{a}_3 + \zeta^2 \mathbf{a}_{3,\alpha} \mathbf{a}_{3,\beta}, \quad g_{\alpha 3} = g_{3\alpha} = 0, \quad g_{33} = 1. \quad (8)$$

The contravariant metric components  $g^{ij}$  can be obtained by the inverse of  $g_{ij}$ , with  $[g^{ij}] = [g_{ij}]^{-1}$ . The constitutive matrices  $\mathbf{D}_0$  and  $\mathbf{D}_2$  are expressed as

$$\mathbf{D}_0 = t \mathbf{D}_{kl}^{(g)}, \quad \mathbf{D}_2 = t^2 \mathbf{D}_{kl}^{(g)} / 12, \quad (9)$$

with

$$\mathbf{D}_{kl}^{(g)} = \frac{E}{1 - \nu^2} \begin{bmatrix} g^{11} g^{11} & \nu g^{11} g^{22} + (1 - \nu) g^{12} g^{12} & g^{11} g^{12} \\ & g^{22} g^{22} & g^{22} g^{12} \\ \text{sym.} & & 0.5[(1 - \nu) g^{11} g^{22} + (1 + \nu) g^{12} g^{12}] \end{bmatrix}. \quad (10)$$

in which  $E$  and  $\nu$  are Young's modulus and Poisson ratio.

For the convenience of sensitivity analysis, the stiffness matrix and external vector given in Eqns. (5)-(6) are re-expressed on the parametric domain, as

$$\mathbf{K}^e = \int_{\bar{\Omega}^e} \left( \mathbf{B}_m^T \mathbf{D}_0 \mathbf{B}_m + \mathbf{B}_b^T \mathbf{D}_2 \mathbf{B}_b \right) |\mathbf{J}| d\bar{\Omega}^e, \quad \mathbf{F}^e = \int_{\bar{\Omega}^e} (\mathbf{R}^e)^T \mathbf{f} |\mathbf{J}| d\bar{\Omega}^e, \quad (11)$$

where  $|\mathbf{J}| = \mathbf{a}_1 \times \mathbf{a}_2 \cdot \mathbf{a}_3 = \|\mathbf{a}_1 \times \mathbf{a}_2\|$ .

### 3 STRUCTURAL OPTIMIZATION

#### 3.1 Problem Definition

The general structural optimization can be generally described as

$$\begin{cases} \text{find } \mathbf{h} \in \mathbb{R}^{n_d} \\ \text{min } f(\mathbf{h}) \\ \text{s.t. } c_i(\mathbf{h}) = 0, \quad \forall i \in \mathcal{E} \\ \quad \quad c_i(\mathbf{h}) \leq 0, \quad \forall i \in \mathcal{I} \end{cases} \quad (12)$$

in which  $\mathbf{h} = [h_1, h_2, \dots, h_{n_d}]^T$  is the design vector;  $n_d$  is the number of design variables;  $f$  is the objective function;  $c_i$  is the constraint;  $\mathcal{E}$  and  $\mathcal{I}$  denote the equality and inequality constraint sets. The objective function can be represented as a function of design variables  $\mathbf{h}$  and field variables  $\mathbf{u}$ , namely,

$$f := f(\mathbf{h}, \mathbf{u}(\mathbf{h})). \quad (13)$$

For linear elastic problems, the relation between  $\mathbf{h}$  and  $\mathbf{u}$  is normally rewritten as

$$\mathbf{K}(\mathbf{h}) \mathbf{u} = \mathbf{F}(\mathbf{h}), \quad (14)$$

where  $\mathbf{K}$  is the stiffness matrix and  $\mathbf{F}$  is the external vector. For Kirchhoff-Love shell structures studied in this paper, they are computed using Eqn. (11).

### 3.2 Adjoint-based Sensitivity

The optimization problem defined in Eqn. (12) can be solved with a variety of algorithms. In this paper, we consider gradient-based optimization algorithms, which present better convergence and computational efficiency when compared to gradient-free methods. The sensitivity analysis is crucial in gradient-based optimization. An analytical adjoint-based method is utilized to compute sensitivity. The derivative of the objective function with respect to the design variables is calculated as

$$\frac{df}{dh_i} = \frac{\partial f}{\partial h_i} + \frac{\partial f}{\partial \mathbf{u}} \frac{d\mathbf{u}}{dh_i}, \quad i = 1, 2, \dots, n_d. \quad (15)$$

The derivative  $d\mathbf{u}/dh_i$  can be recovered from Eqn. (14). Then the above equation can be rewritten as

$$\frac{df}{dh_i} = \frac{\partial f}{\partial h_i} + \frac{\partial f}{\partial \mathbf{u}} \mathbf{K}^{-1} \left( \frac{\partial \mathbf{F}}{\partial h_i} - \frac{\partial \mathbf{K}}{\partial h_i} \mathbf{u} \right), \quad i = 1, 2, \dots, n_d. \quad (16)$$

Introducing an adjoint solution  $\mathbf{u}^*$ , with

$$\mathbf{K} \mathbf{u}^* = \left( \frac{\partial f}{\partial \mathbf{u}} \right)^T, \quad (17)$$

to Eqn. (16), we can find

$$\frac{df}{dh_i} = \frac{\partial f}{\partial h_i} + \mathbf{u}^* \left( \frac{\partial \mathbf{F}}{\partial h_i} - \frac{\partial \mathbf{K}}{\partial h_i} \mathbf{u} \right), \quad i = 1, 2, \dots, n_d. \quad (18)$$

It can be found that the adjoint solution is solved only once for each sensitivity analysis. The entire process is more efficient for problems with fewer constraints. In shape optimization, the sensitivity analysis of design variables is transformed to compute the sensitivity of control points. Let  $\mathbf{P}$  be the control points of the design model, Eqn. (18) can be rewritten as

$$\frac{df}{dh_i} = \frac{\partial f}{\partial h_i} + \left( \mathbf{u}^* \frac{\partial \mathbf{F}}{\partial \mathbf{P}} - \mathbf{u}^* \frac{\partial \mathbf{K} \mathbf{u}}{\partial \mathbf{P}} \right) \frac{\partial \mathbf{P}}{\partial h_i}, \quad i = 1, 2, \dots, n_d. \quad (19)$$

### 3.3 Multi-level Scheme

Note that the geometric model can be precisely refined in IGA, we can construct a multi-level model for structural optimization with a coarse-level model for geometric design and a dense-level model for numerical analysis. Fig. 1 shows the process of isogeometric structural optimization based on a multi-level model. The multi-level strategy is important in structural optimization. For instance, the design model generally requires fewer control points to avoid the perturbation of optimized geometric shape in shape optimization. However, for structural analysis, more control points are usually required to improve the computational accuracy.

Let  $\mathbf{Q}$  be the control points of dense models for structural analysis. There is a linear mapping between  $\mathbf{P}$  and  $\mathbf{Q}$ , written as  $\mathbf{Q} = \mathbf{M} \mathbf{P}$ . The matrix  $\mathbf{M}$  can be obtained using the classical knot insertion algorithm. Correspondingly, the derivative of any function  $(\cdot)$  with respect to the control points  $\mathbf{P}$  can be given by

$$\frac{\partial(\cdot)}{\partial \mathbf{P}} = \frac{\partial(\cdot)}{\partial \mathbf{Q}} \frac{\partial \mathbf{Q}}{\partial \mathbf{P}} = \frac{\partial(\cdot)}{\partial \mathbf{Q}} \mathbf{M}. \quad (20)$$

Combining Eqns. (19) and (20), leads to

$$\frac{df}{dh_i} = \frac{\partial f}{\partial h_i} + \left( \mathbf{u}^* \frac{\partial \mathbf{F}}{\partial \mathbf{Q}} - \mathbf{u}^* \frac{\partial \mathbf{K} \mathbf{u}}{\partial \mathbf{Q}} \right) \mathbf{M} \frac{\partial \mathbf{P}}{\partial h_i}, \quad i = 1, 2, \dots, n_d. \quad (21)$$

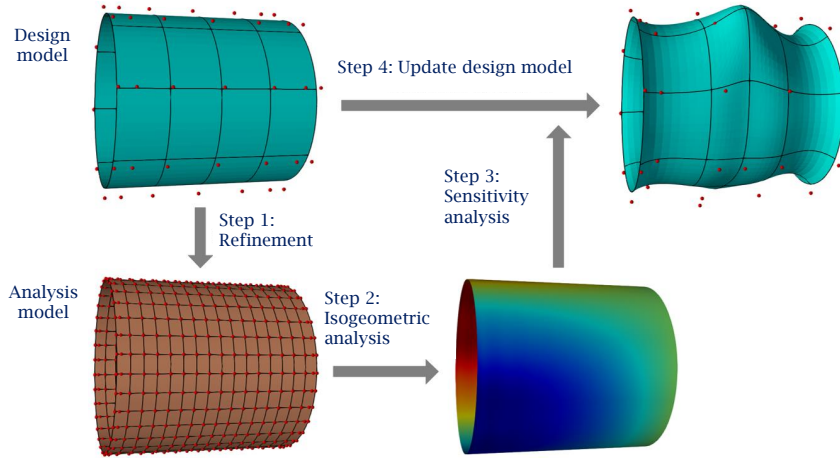


**Figure 1:** The process of isogeometric structural optimization using a multi-level model.

The total energy of a linear elastic system can be defined as

$$\mathcal{W}(\mathbf{u}, \mathbf{u}^*, \mathbf{Q}) = \mathcal{W}_{ext}(\mathbf{u}^*, \mathbf{Q}) + \mathcal{W}_{int}(\mathbf{u}, \mathbf{u}^*, \mathbf{Q}) = \mathbf{u}^* \mathbf{F} - \mathbf{u}^* \mathbf{K} \mathbf{u}. \quad (22)$$

Then the derivative in Eqn. (21) is simplified as

$$\frac{df}{dh_i} = \frac{\partial f}{\partial h_i} + \frac{\partial \mathcal{W}}{\partial \mathbf{Q}} \mathbf{M} \frac{\partial \mathbf{P}}{\partial h_i}, \quad i = 1, 2, \dots, n_d, \quad (23)$$

in which the term  $\partial \mathbf{P} / \partial h_i$  can be obtained in the construction of design model. The remaining unknown term is  $\partial \mathcal{W} / \partial \mathbf{Q}$ , which is related to the structural responses.

## 4 ISOGOMETRIC SHAPE AND TOPOLOGY OPTIMIZATION

### 4.1 Optimization Problem Definition

Considering the minimization of compliance under the constraints of volume, the shape optimization on the design domain  $\Omega$  is defined as

$$\left\{ \begin{array}{l} \text{find } \mathbf{h} \in \mathbb{R}^{n_d} \\ \text{min } f(\mathbf{h}) := \mathbf{F}^T \mathbf{u} \\ \text{s.t. } \mathbf{K}(\mathbf{h}) \mathbf{u} = \mathbf{F}, \\ \quad g(\mathbf{h}) := V(\mathbf{h}) / V_0 - \gamma \leq 0, \\ \quad \underline{h}_i \leq h_i \leq \overline{h}_i, \quad i = 1, 2, \dots, n_d, \end{array} \right. \quad (24)$$

where  $\mathbf{h} = [h_1, h_2, \dots, h_{n_d}]^T$  denotes the design variables corresponding to the geometric shape of the design domain;  $V_0$  denotes the initial area of the design domain;  $V(\mathbf{h})$  indicates the area of the current  $\mathbf{h}$ ;  $\gamma$  is the prescribed volume fraction;  $g$  is the volume constraint function;  $\underline{h}_i$  and  $\overline{h}_i$  are the lower and upper bounds of the variable  $h_i$ .

Similarly, the topology optimization considering the minimization of compliance is defined as

$$\left\{ \begin{array}{l} \text{find } \mathbf{h} \in \mathbb{R}^{n_d} \\ \text{min } f(\chi(\mathbf{h})) := \mathbf{F}^T \mathbf{u} \\ \text{s.t. } \mathbf{K}(\chi) \mathbf{u} = \mathbf{F}, \\ g(\chi) := \frac{1}{V_0} \int_{\Omega} \chi d\Omega - \gamma \leq 0, \\ 0 \leq h_i \leq 1, \quad i = 1, 2, \dots, n_d, \end{array} \right. \quad (25)$$

in which  $\chi(\mathbf{h})$  indicates the density distribution of material.

## 4.2 Sensitivity Analysis of Shape Optimization

In isogeometric shape optimization, the sensitivity analysis with respect to the design variables can be generally transformed into the sensitivity analysis with respect to the control points. According to the definition of the objective function in Eqn. (24), the adjoint vector  $\mathbf{u}^*$  is equal to the displacement  $\mathbf{u}$ . Therefore, it is unnecessary to solve the adjoint problem defined in Eqn. (17). The derivatives of external work  $\mathcal{W}_{ext}$  and internal work  $\mathcal{W}_{int}$  w.r.t. control points  $Q_{aj}$ , read as

$$\frac{\partial \mathcal{W}_{ext}}{\partial Q_{aj}^e} = \mathbf{u}^e \frac{\partial \mathbf{F}^e}{\partial Q_{aj}^e}, \quad \frac{\partial \mathcal{W}_{int}}{\partial Q_{aj}^e} = -\mathbf{u}^e \frac{\partial \mathbf{K}^e}{\partial Q_{aj}^e} \mathbf{u}^e, \quad e = 1, 2, \dots, m_e, \quad a = 1, 2, \dots, m_{cp}^e, \quad j = 1, 2, 3. \quad (26)$$

The term  $Q_{aj}^e$  denotes the  $j$ -th component of the  $a$ -th control point for the element  $e$ . Considering the expressions of the stiffness matrix and external force vector given in Eqn. (11), the terms  $\frac{\partial \mathbf{F}^e}{\partial Q_{aj}^e}$  and  $\frac{\partial \mathbf{K}^e}{\partial Q_{aj}^e}$  in the above equation can be computed by

$$\frac{\partial \mathbf{F}^e}{\partial Q_{aj}^e} = \int_{\Omega^e} (\mathbf{R}^e)^T \mathbf{f} \frac{\partial |\mathbf{J}|}{\partial Q_{aj}^e} d\bar{\Omega}^e, \quad (27)$$

$$\begin{aligned} \frac{\partial \mathbf{K}^e}{\partial Q_{aj}^e} &= \int_{\Omega^e} \left( \frac{\partial \mathbf{B}_m^T}{\partial Q_{aj}^e} \mathbf{D}_0 \mathbf{B}_m + \mathbf{B}_m^T \frac{\partial \mathbf{D}_0}{\partial Q_{aj}^e} \mathbf{B}_m + \mathbf{B}_m^T \mathbf{D}_0 \frac{\partial \mathbf{B}_m}{\partial Q_{aj}^e} \right) |\mathbf{J}| d\bar{\Omega}^e \\ &+ \int_{\Omega^e} \left( \frac{\partial \mathbf{B}_b^T}{\partial Q_{aj}^e} \mathbf{D}_2 \mathbf{B}_b + \mathbf{B}_b^T \frac{\partial \mathbf{D}_2}{\partial Q_{aj}^e} \mathbf{B}_b + \mathbf{B}_b^T \mathbf{D}_2 \frac{\partial \mathbf{B}_b}{\partial Q_{aj}^e} \right) |\mathbf{J}| d\bar{\Omega}^e \\ &+ \int_{\bar{\Omega}^e} \left( \mathbf{B}_m^T \mathbf{D}_0 \mathbf{B}_m + \mathbf{B}_b^T \mathbf{D}_2 \mathbf{B}_b \right) \frac{\partial |\mathbf{J}|}{\partial Q_{aj}^e} d\bar{\Omega}^e. \end{aligned} \quad (28)$$

## 4.3 Density Distribution and Sensitivity of Topology Optimization

The density method is employed for topology optimization of shell structures. Different from the shape optimization, the design variables  $\mathbf{h}$  will affect the mechanical behaviors through the density distribution function in the topology optimization. Assume that each control point has a density parameter  $h_i \in [0, 1], i = 1, 2, \dots, n_d$ , the density distribution can be described as

$$\chi^e(\xi, \eta) = \sum_{a=1}^{m_{cp}^e} \rho_a^e R_a^e(\xi, \eta), \quad (\xi, \eta) \in \bar{\Omega}^e, \quad e = 1, 2, \dots, m_e, \quad (29)$$

where  $\rho_a^e$  indicates the density of the  $a$ -th control point of element  $e$ . According to the SIMP interpolation method, the Young's modulus  $E^e(\chi^e(\xi, \eta))$  can be expressed by

$$E^e(\chi^e(\xi, \eta)) = E_{min} + [\chi^e(\xi, \eta)]^s (E_0 - E_{min}), \quad (30)$$

in which  $E_0$  is the Young's modulus of the model;  $E_{min}$  is a small value to avoid singularity of the stiffness matrix,  $s$  is a penalization power.

In sensitivity analysis, the derivative of the stiffness matrix *w.r.t.* the density of control points is given by

$$\frac{\partial \mathbf{K}^e}{\partial \rho_a^e} = \int_{\bar{\Omega}^e} \left( t \mathbf{B}_m^T \frac{\partial \mathbf{D}_{kl}^g}{\partial \rho_a^e} \mathbf{B}_m + \frac{t^3}{12} \mathbf{B}_b^T \frac{\partial \mathbf{D}_{kl}^g}{\partial \rho_a^e} \mathbf{B}_b \right) |\mathbf{J}| d\bar{\Omega}^e. \quad (31)$$

## 5 NUMERICAL EXAMPLES

### 5.1 Shape Optimization of A L-shaped Shell

An L-shaped shell model with a central hole is taken as the design domain for shape optimization in this example. As shown in Fig. 2(a), the top edge is fixed and the bottom edge is subjected to a uniform line load  $F = 1$ . For the material properties, Young's modulus  $E = 6.825 \times 10^7$ , Poisson ratio  $\nu = 0.3$ . The thickness of the shell takes  $t = 0.04$ . It can be observed that there are several extraordinary points in the design model.

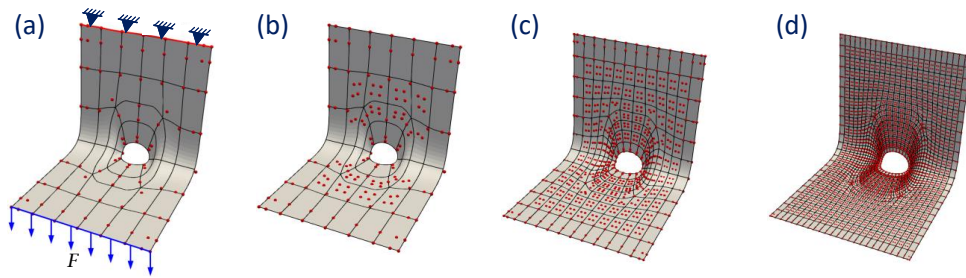


**Figure 2:** The L-shaped shell model with a central hole. (a) Design model  $S_{D0}$  with boundary conditions, (b) analysis model  $S_{A0}$  and the refined analysis model (c)  $S_{A1}$ , (d)  $S_{A2}$ .

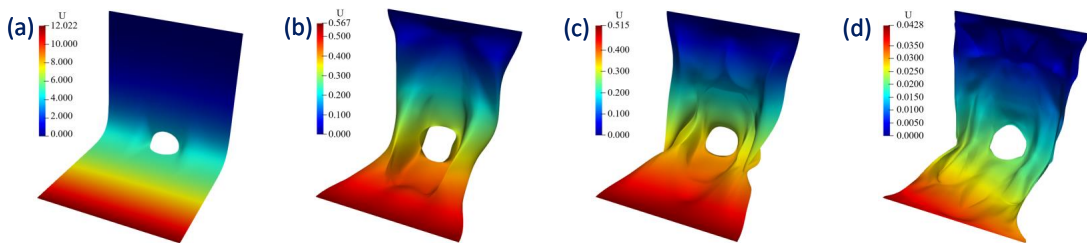


**Figure 3:** The isogeometric analysis results for (a) initial design model with compliance of 182.601, (b) optimized shape using scheme #1, with compliance of 8.7043, (c) optimized shape using scheme #2, with compliance of 7.2267, and (d) optimized shape using scheme #3, with compliance of 1.0399.

To satisfy the  $C^1$  continuity requirement for the Kirchhoff-Love shell, the analysis model  $S_{A0}$  as given in Fig. 2(b) is constructed from the design model  $S_{D0}$  using the D-patch scheme. Then the initial analysis model is refined twice to get the dense models  $S_{A1}$  and  $S_{A2}$ , as shown in Figs. 2(c) and 2(d). The geometric



shape of the four surfaces is the same with each other. The number of control points is 104, 176, 720 and 2960. Three multi-level schemes are designed as follows

- Scheme #1: Taking  $S_{D0}$  as the design model and  $S_{A2}$  as the analysis model.
- Scheme #2: Taking  $S_{A0}$  as the design model and  $S_{A2}$  as the analysis model.
- Scheme #3: Taking  $S_{A1}$  as the design model and  $S_{A2}$  as the analysis model.

In each scheme, the two-layer boundary control points are constrained and the coordinates of central control points are treated as the design variables. The classical MMA algorithm [33] combined with the open-source library NLOpt [17] is used to update the design variables.

Fig. 3 illustrates the isogeometric results of the initial model and the optimized models. It can be found that the compliance values of the three optimized models are 8.7043, 7.2267 and 1.0399, which are much lower than that of the initial model 182.601. However, the geometric shape of the three optimized models is different. More control points in the design model will lead to more details on the optimized model, which can be observed from Fig. 3(d). Although scheme #3 presents the lowest compliance, there are plenty of wrinkles on the model and the surface quality is poor. The optimized model obtained by using schemes #2 and #3 is relatively reasonable and is smoother than that of #1. The convergence curves of the isogeometric shape optimization for three schemes are demonstrated in Fig. 4. The objective functions for all three schemes can converge fast to stable values.

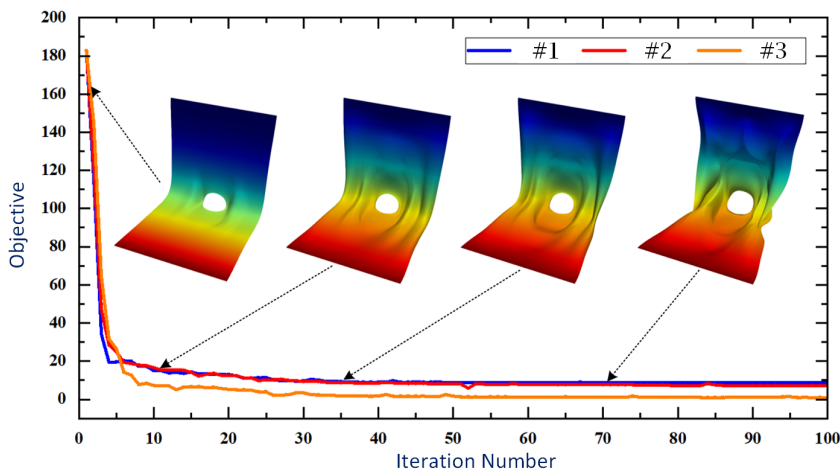


**Figure 4:** The convergence curve for the isogeometric shape optimization of the L-shaped shell using three schemes #1, #2, and #3.

## 5.2 Shape Optimization of A Blend Surface Shell

The shape optimization of a blend surface shell is studied in this example, as depicted in Fig. 5(a). The blend surface shell is constructed by blending three basis surfaces with six control parameters  $\alpha_1, \alpha_2, \alpha_3, \beta_1, \beta_2, \beta_3$  developed by Yang et al. [37]. Two bottom boundary edges are fixed. The top edge is subjected to two types of forces: one is horizontal and the other is vertical. The magnitudes of the two forces are 1. The Young's modulus  $E = 3 \times 10^6$  and Poisson ratio  $\nu = 0.3$ , thickness of the roof  $t = 0.1$ . The volume fraction of the shell is assumed to be 100%, namely, no change on the shell surface area. To improve the accuracy of

the computation of structural responses, the design model is refined as given in Fig. 5(b). Two schemes are formulated to select design variables as follows:

- Scheme #1: The six design parameters related to the green control points and the coordinates of the blue control points are selected as design variables, as shown in Fig. 5(c).
- Scheme #2: The coordinates of the blue control points, as shown in Fig. 5(d), are selected as design variables.

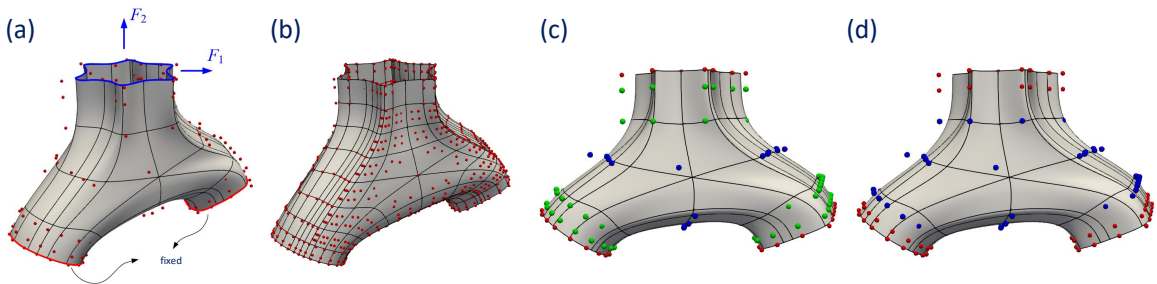


**Figure 5:** The blend shell model. (a) The design model and boundary conditions; (b) The analysis model refined from the design model; (c) Scheme #1, the blue control points move freely and the green control points are controlled by design parameters of the blend surface; (d) Scheme #2, the blue control points move freely.

The shape optimization results are illustrated in Fig. 6. Figs. 6(a) and 6(d) present the displacement results of the initial design under two different force conditions. The optimized shapes using scheme #1 are given in the sub-figures 6(b) and 6(e). The sub-figures 6(c) and 6(f) show the optimized shapes using scheme #2. It is observed that both schemes achieve lower compliance under two types of force conditions. Scheme #2 produces lower compliance but more surface defects including fold, twist and self-crossing, which are considered to be caused by more design variables. The optimization history of the blend shell model based on schemes #1 and #2 under two force conditions is plotted in Fig. 7, where the convergence curve of scheme #2 fluctuates more sharply.

### 5.3 Topology Optimization of A Bracket

In this example, we consider the isogeometric topology optimization of a connecting bracket of the payload adapter of the LISA Pathfinder satellite [1]. The geometric model of the bracket is simplified as shown in Fig. 8. The model is constructed using ASUT-splines as illustrated in Fig. 9. The red domain in Fig. 9(a) is selected as the undesigned domain. The top face is subjected to a uniform load and the bottom face panels are fixed as illustrated in Fig. 9(b). The material takes aluminium alloy Al7075 with Young's modulus  $E = 70.3\text{GPa}$ , Poisson ratio  $\nu = 0.33$ . The initial design model is globally refined twice with 6572 elements for simulation.

The volume fraction and density of the initial control points take 0.8. The displacement results of the initial model and the optimized model are plotted in Figs. 9(c) and 9(d). It can be found that the maximum displacement rises from 0.4918 to 0.4948 by 0.61%. Fig. 10 presents the optimization history of the compliance of the bracket. The four history configurations correspond to the 1, 7, 10 and 100 steps. The compliance is reduced from 26.574 to 9.521. The surface area is reduced to 80% of the original area.

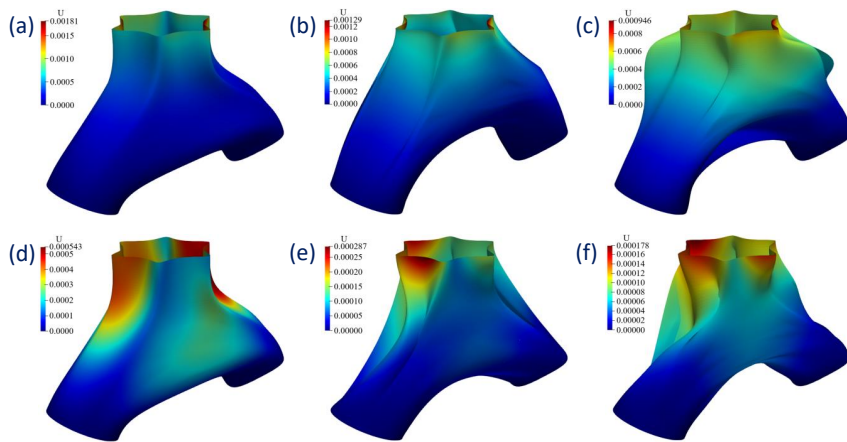


**Figure 6:** The shape optimization of blend shell. (a) Force 1, initial design, obj (compliance) = 0.030944; (b) Force 1, optimized design by scheme #1, obj = 0.020844; (c) Force 1, optimized design by scheme #2, obj = 0.015684; (d) Force 2, initial design, obj = 0.0086497; (e) Force 2, optimized design by scheme #1, obj = 0.0039623; (f) Force 2, optimized design by scheme #2, obj = 0.0034172.

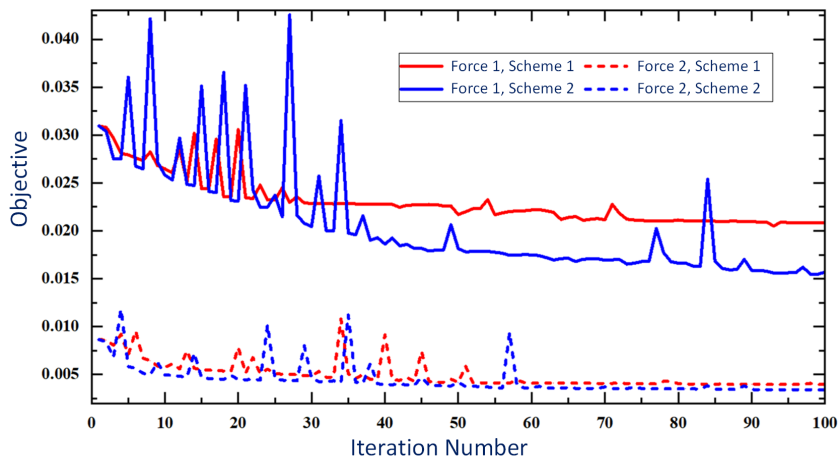


**Figure 7:** The optimization history of the blend shell model based on schemes #1 and #2 under two force conditions.

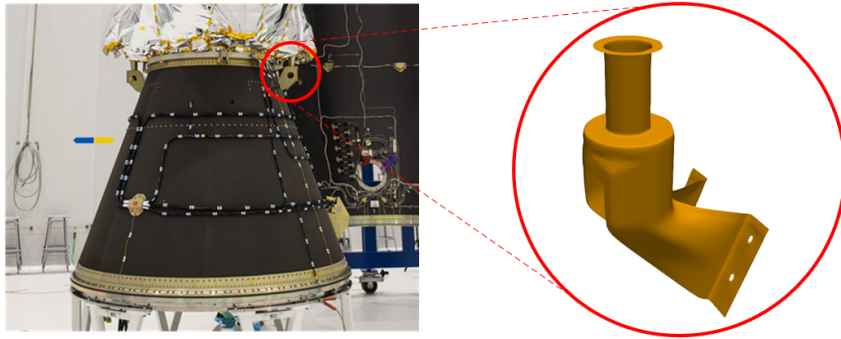


**Figure 8:** The bracket of payload adapter on the LISA Pathfinder [1] and its simplified geometric model.

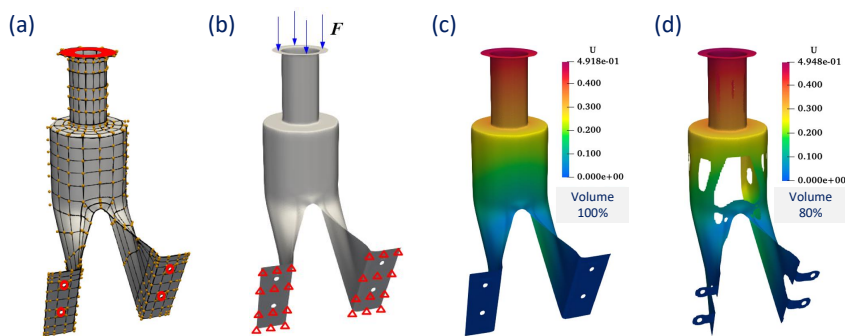


**Figure 9:** The geometric modeling and topology optimization of the bracket. (a) ASUT-spline based modeling; (b) Boundary conditions; (c) and (d) The isogeometric analysis of the initial and optimized models.

## 6 CONCLUSIONS

A unified geometric data is the cornerstone for IGA-based structural optimization. Other than traditionally using NURBS to implement shape representation, analysis as well as optimization, this paper constructs a complete framework to capacitate the relevant operations on the basis of ASUT-splines. The necessary technology details to realize shape and topology optimization are explained and the whole process indicates the potential for combining IGA with unstructured splines to underpin an integrated CAD/CAE/OPT scenario. From the numerical examples, it is observed that the increase of control points in the design model may deteriorate the optimization results. Therefore, the design model should be chosen carefully with a suitable refinement. For the future perspective, the shape and topology optimization around the neighboring area of extraordinary points require more investigation.

## ACKNOWLEDGEMENTS

The work is supported by Beijing Natural Science Foundation (Project No. 4242025), National Natural Science Foundation of China (Project Nos. 62102012, 52175213 and 61972011) and Young Elite Scientists Sponsorship Program by CAST (Project No. 2022QNRC001) as well as \*\*\*\* Computer aided design \*\*\*\* for design tool chain project.

Xiaoxiao Du, <https://orcid.org/0000-0002-2324-1005>

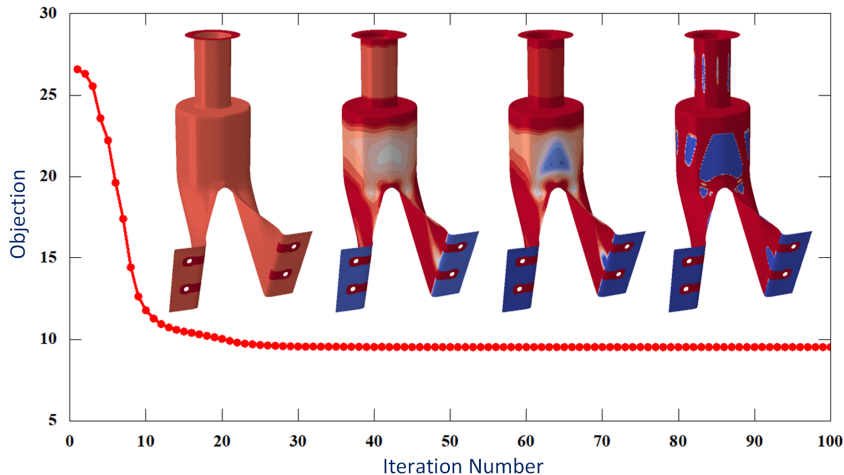


**Figure 10:** The optimization history of compliance of the bracket and four middle configurations.

## REFERENCES

- [1] LISA Pathfinder being encapsulated within the fairing. <https://sci.esa.int/web/lisa-pathfinder/-/56979-lisa-pathfinder-being-encapsulated-within-the-fairing>.
- [2] Bandara, K.; Cirak, F.: Isogeometric shape optimisation of shell structures using multiresolution subdivision surfaces. *Computer-Aided Design*, 95, 62–71, 2018. <http://doi.org/10.17863/CAM.22608>.
- [3] Bletzinger, K.U.; Wüchner, R.; Daoud, F.; Camprubí, N.: Computational methods for form finding and optimization of shells and membranes. *Computer methods in applied mechanics and engineering*, 194(30-33), 3438–3452, 2005. <http://doi.org/10.1016/j.cma.2004.12.026>.
- [4] Cai, S.; Zhang, H.; Zhang, W.: An integrated design approach for simultaneous shape and topology optimization of shell structures. *Computer Methods in Applied Mechanics and Engineering*, 415, 116218, 2023. <http://doi.org/10.1016/j.cma.2023.116218>.
- [5] Casquero, H.; Wei, X.; Toshniwal, D.; Li, A.; Hughes, T.J.; Kiendl, J.; Zhang, Y.J.: Seamless integration of design and Kirchhoff–Love shell analysis using analysis-suitable unstructured T-splines. *Computer Methods in Applied Mechanics and Engineering*, 360, 112765, 2020. <http://doi.org/10.1016/j.cma.2019.112765>.
- [6] Chen, L.; Zhang, W.; Meng, L.; Jiu, L.; Feng, S.: An adaptive T-spline finite cell method for structural shape optimization. *Structural and Multidisciplinary Optimization*, 61, 1857–1876, 2020. <http://doi.org/10.1007/s00158-020-02645-w>.
- [7] Ding, C.; Cui, X.; Huang, G.; Li, G.; Tamma, K.; Cai, Y.: A gradient-based shape optimization scheme via isogeometric exact reanalysis. *Engineering Computations*, 35(8), 2696–2721, 2018. <http://doi.org/10.1108/EC-08-2017-0292>.
- [8] Du, X.; Zhang, R.; Wang, W.; Zhao, G.; Liu, Y.: Multi-patch isogeometric Kirchhoff–Love shell analysis for post-buckling of functionally graded graphene platelets reinforced composite shells. *Thin-Walled Structures*, 196, 111470, 2024. <http://doi.org/10.1016/j.tws.2023.111470>.
- [9] Du, X.; Zhao, G.; Wang, W.; Fang, H.: Nitsche’s method for non-conforming multipatch coupling in hyperelastic isogeometric analysis. *Computational Mechanics*, 65, 687–710, 2020. <http://doi.org/10.1007/s00466-019-01789-x>.

- [10] Du, X.; Zhao, G.; Wang, W.; Guo, M.; Zhang, R.; Yang, J.: Triangular and quadrilateral Bézier discretizations of trimmed CAD surfaces and its application to the isogeometric analysis. *Computer-Aided Design & Applications*, 18(4), 2021. <http://doi.org/10.14733/cadconfP.2020.147-151>.
- [11] Du, X.; Zhao, G.; Wang, W.; Liu, Y.; Zhang, P.; Han, P.; Cheng, H.: Parametric modeling and simulation of a simplified horizontal tail under the framework of isogeometric analysis. *Computer-Aided Design and Applications*, 21(4), 635–645, 2024. <http://doi.org/10.14733/cadaps.2024.635-645>.
- [12] Du, X.; Zhao, G.; Zhang, R.; Wang, W.; Yang, J.: Numerical implementation for isogeometric analysis of thin-walled structures based on a Bézier extraction framework: nligaStruct. *Thin-Walled Structures*, 180, 109844, 2022. <http://doi.org/10.1016/j.tws.2022.109844>.
- [13] Guo, M.; Wang, W.; Zhao, G.; Du, X.; Zhang, R.; Yang, J.: T-Splines for isogeometric analysis of the large deformation of elastoplastic Kirchhoff–Love shells. *Applied Sciences*, 13(3), 1709, 2023. <http://doi.org/10.3390/app13031709>.
- [14] Hao, P.; Liu, X.; Wang, Y.; Liu, D.; Wang, B.; Li, G.: Collaborative design of fiber path and shape for complex composite shells based on isogeometric analysis. *Computer Methods in Applied Mechanics and Engineering*, 354, 181–212, 2019. <http://doi.org/10.1016/j.cma.2019.05.044>.
- [15] Hirschler, T.; Bouclier, R.; Duval, A.; Elguedj, T.; Morlier, J.: The embedded isogeometric Kirchhoff–Love shell: From design to shape optimization of non-conforming stiffened multipatch structures. *Computer Methods in Applied Mechanics and Engineering*, 349, 774–797, 2019. <http://doi.org/10.1016/j.cma.2019.02.042>.
- [16] Hughes, T.J.; Cottrell, J.A.; Bazilevs, Y.: Isogeometric analysis: CAD, finite elements, NURBS, exact geometry and mesh refinement. *Computer methods in applied mechanics and engineering*, 194(39-41), 4135–4195, 2005. <http://doi.org/10.1016/j.cma.2004.10.008>.
- [17] Johnson, S.G.: The NLOpt nonlinear-optimization package. <https://github.com/stevengj/nlopt>, 2007.
- [18] Kang, P.; Youn, S.K.: Isogeometric shape optimization of trimmed shell structures. *Structural and Multidisciplinary Optimization*, 53, 825–845, 2016. <http://doi.org/10.1016/j.finel.2016.06.003>.
- [19] Kang, P.; Youn, S.K.: Isogeometric topology optimization of shell structures using trimmed NURBS surfaces. *Finite Elements in Analysis and Design*, 120, 18–40, 2016. <http://doi.org/10.1016/j.finel.2016.06.003>.
- [20] Kiendl, J.; Schmidt, R.; Wüchner, R.; Bletzinger, K.U.: Isogeometric shape optimization of shells using semi-analytical sensitivity analysis and sensitivity weighting. *Computer Methods in Applied Mechanics and Engineering*, 274, 148–167, 2014. <http://doi.org/10.1016/j.cma.2014.02.001>.
- [21] Li, X.; Zheng, J.; Sederberg, T.W.; Hughes, T.J.; Scott, M.A.: On linear independence of T-spline blending functions. *Computer Aided Geometric Design*, 29(1), 63–76, 2012. <http://doi.org/10.1016/j.cagd.2011.08.005>.
- [22] Lian, H.; Kerfriden, P.; Bordas, S.: Shape optimization directly from CAD: An isogeometric boundary element approach using T-splines. *Computer Methods in Applied Mechanics and Engineering*, 317, 1–41, 2017. <http://doi.org/10.1016/j.cma.2016.11.012>.
- [23] Liguori, F.S.; Zucco, G.; Madeo, A.; Garcea, G.; Leonetti, L.; Weaver, P.M.: An isogeometric framework for the optimal design of variable stiffness shells undergoing large deformations. *International Journal of Solids and Structures*, 210, 18–34, 2021. <http://doi.org/10.1016/j.ijsolstr.2020.11.003>.
- [24] Liu, Z.; Cheng, J.; Yang, M.; Yuan, P.; Qiu, C.; Gao, W.; Tan, J.: Isogeometric analysis of large thin shell structures based on weak coupling of substructures with unstructured T-splines patches. *Advances in Engineering Software*, 135, 102692, 2019. <http://doi.org/10.1016/j.advengsoft.2019.102692>.

- [25] López, J.; Anitescu, C.; Rabczuk, T.: Isogeometric structural shape optimization using automatic sensitivity analysis. *Applied Mathematical Modelling*, 89, 1004–1024, 2021. <http://doi.org/10.1016/j.apm.2020.07.027>.
- [26] Maute, K.; Ramm, E.: Adaptive topology optimization of shell structures. *AIAA journal*, 35(11), 1767–1773, 1997. <http://doi.org/doi.org/10.2514/2.25>.
- [27] Nagy, A.P.; IJsselmuiden, S.T.; Abdalla, M.M.: Isogeometric design of anisotropic shells: optimal form and material distribution. *Computer Methods in Applied Mechanics and Engineering*, 264, 145–162, 2013. <http://doi.org/10.1016/j.cma.2013.05.019>.
- [28] Nguyen, T.; Peters, J.: Refinable C1 spline elements for irregular quad layout. *Computer aided geometric design*, 43, 123–130, 2016. <http://doi.org/10.1016/j.cagd.2016.02.009>.
- [29] Pan, Q.; Zhai, X.; Chen, F.: Density-based isogeometric topology optimization of shell structures. *arXiv preprint arXiv:2312.06378*, 2023. <http://doi.org/10.48550/arXiv.2312.06378>.
- [30] Reif, U.: A refineable space of smooth spline surfaces of arbitrary topological genus. *Journal of Approximation Theory*, 90(2), 174–199, 1997. <http://doi.org/10.1006/jath.1996.3079>.
- [31] Scott, M.A.; Simpson, R.N.; Evans, J.A.; Lipton, S.; Bordas, S.P.; Hughes, T.J.; Sederberg, T.W.: Isogeometric boundary element analysis using unstructured T-splines. *Computer Methods in Applied Mechanics and Engineering*, 254, 197–221, 2013. <http://doi.org/10.1016/j.cma.2012.11.001>.
- [32] Seo, Y.D.; Kim, H.J.; Youn, S.K.: Shape optimization and its extension to topological design based on isogeometric analysis. *International Journal of Solids and Structures*, 47(11-12), 1618–1640, 2010. <http://doi.org/10.1016/j.ijsolstr.2010.03.004>.
- [33] Svanberg, K.: A class of globally convergent optimization methods based on conservative convex separable approximations. *SIAM Journal on Optimization*, 12(2), 555–573, 2002.
- [34] Toshniwal, D.; Speleers, H.; Hughes, T.J.: Smooth cubic spline spaces on unstructured quadrilateral meshes with particular emphasis on extraordinary points: Geometric design and isogeometric analysis considerations. *Computer Methods in Applied Mechanics and Engineering*, 327, 411–458, 2017. <http://doi.org/10.1016/j.cma.2017.06.008>.
- [35] Wei, X.; Li, X.; Qian, K.; Hughes, T.J.; Zhang, Y.J.; Casquero, H.: Analysis-suitable unstructured T-splines: Multiple extraordinary points per face. *Computer Methods in Applied Mechanics and Engineering*, 391, 114494, 2022. <http://doi.org/10.1016/j.cma.2021.114494>.
- [36] Yang, F.; Yu, T.; Liu, Z.; Bui, T.Q.: Isogeometric double-objective shape optimization of free-form surface structures with Kirchhoff–Love shell theory. *Finite Elements in Analysis and Design*, 223, 103989, 2023. <http://doi.org/10.1016/j.finel.2023.103989>.
- [37] Yang, J.; Zhao, G.; Wang, W.; Du, X.; Guo, M.; Zhang, R.: Surface blending using T-splines in semi-NURBS form. *Computer-Aided Design*, 146, 103210, 2022. <http://doi.org/10.1016/j.cad.2022.103210>.
- [38] Yang, J.; Zhao, G.; Wang, W.; Du, X.; Zuo, C.: Non-uniform C1 patches around extraordinary points with applications to analysis-suitable unstructured T-splines. *Computer Methods in Applied Mechanics and Engineering*, 405, 115849, 2023. <http://doi.org/10.1016/j.cma.2022.115849>.
- [39] Yin, S.; Huang, J.; Zou, Z.; Bui, T.Q.; Cong, Y.; Yu, T.; Zhang, G.: Isogeometric shape optimization for widening band gaps of periodic composite plates. *European Journal of Mechanics-A/Solids*, 103, 105142, 2024. <http://doi.org/10.1016/j.euromechsol.2023.105142>.
- [40] Zhang, W.; Jiang, S.; Liu, C.; Li, D.; Kang, P.; Youn, S.K.; Guo, X.: Stress-related topology optimization of shell structures using IGA/TSA-based moving morphable void (MMV) approach. *Computer Methods in Applied Mechanics and Engineering*, 366, 113036, 2020. <http://doi.org/10.1016/j.cma.2020.113036>.

- [41] Zhang, W.; Li, D.; Kang, P.; Guo, X.; Youn, S.K.: Explicit topology optimization using IGA-based moving morphable void (MMV) approach. *Computer Methods in Applied Mechanics and Engineering*, 360, 112685, 2020. <http://doi.org/10.1016/j.cma.2019.112685>.
- [42] Zhao, G.; Yang, J.; Wang, W.; Zhang, Y.; Du, X.; Guo, M.: T-splines based isogeometric topology optimization with arbitrarily shaped design domains. *Computer Modeling in Engineering & Sciences*, 123(3), 1033–1059, 2020. <http://doi.org/10.32604/cmescs.2020.09920>.
- [43] Zhong, S.; Jin, G.; Ye, T.: Isogeometric vibration and material optimization of rotating in-plane functionally graded thin-shell blades with variable thickness. *Thin-Walled Structures*, 185, 110593, 2023. <http://doi.org/10.1016/j.tws.2023.110593>.